

## MIT Open Access Articles

*High-Fat Diet Triggers Inflammation-Induced Cleavage of SIRT1 in Adipose Tissue To Promote Metabolic Dysfunction*

The MIT Faculty has made this article openly available. **Please share** how this access benefits you. Your story matters.

**Citation:** Chalkiadaki, Angeliki, and Leonard Guarente. "High-Fat Diet Triggers Inflammation-Induced Cleavage of SIRT1 in Adipose Tissue To Promote Metabolic Dysfunction." *Cell Metabolism* 16, no. 2 (August 2012): 180–188. © 2012 Elsevier Inc.

**As Published:** <http://dx.doi.org/10.1016/j.cmet.2012.07.003>

**Publisher:** Elsevier

**Persistent URL:** <http://hdl.handle.net/1721.1/91624>

**Version:** Final published version: final published article, as it appeared in a journal, conference proceedings, or other formally published context

**Terms of Use:** Article is made available in accordance with the publisher's policy and may be subject to US copyright law. Please refer to the publisher's site for terms of use.



# High-Fat Diet Triggers Inflammation-Induced Cleavage of SIRT1 in Adipose Tissue To Promote Metabolic Dysfunction

Angeliki Chalkiadaki<sup>1</sup> and Leonard Guarente<sup>1,\*</sup>

<sup>1</sup>Paul F. Glenn Laboratory and Department of Biology, Massachusetts Institute of Technology, Cambridge MA 02139, USA

\*Correspondence: leng@mit.edu

<http://dx.doi.org/10.1016/j.cmet.2012.07.003>

## SUMMARY

Adipose tissue plays an important role in storing excess nutrients and preventing ectopic lipid accumulation in other organs. Obesity leads to excess lipid storage in adipocytes, resulting in the generation of stress signals and the derangement of metabolic functions. SIRT1 is an important regulatory sensor of nutrient availability in many metabolic tissues. Here we report that SIRT1 functions in adipose tissue to protect from inflammation and obesity under normal feeding conditions, and to forestall the progression to metabolic dysfunction under dietary stress and aging. Genetic ablation of *SIRT1* in adipose tissue leads to gene expression changes that highly overlap with changes induced by high-fat diet in wild-type mice, suggesting that dietary stress signals inhibit the activity of SIRT1. Indeed, we show that high-fat diet induces the cleavage of SIRT1 protein in adipose tissue by the inflammation-activated caspase-1, providing a link between dietary stress and predisposition to metabolic dysfunction.

## INTRODUCTION

Obesity is associated with the pathological condition of insulin resistance, which often leads to a number of interrelated metabolic derangements, including liver steatosis, hyperlipidemia, glucose intolerance, and cardiovascular disease, collectively characterized as the metabolic syndrome. Central to the development of the metabolic syndrome is white adipose tissue, which serves as the primary lipid storage depot. Excess caloric intake results in hypertrophic and dysfunctional adipocytes (Qatanani and Lazar, 2007; Rosen and Spiegelman, 2006). Increased intracellular lipid accumulation activates several stress pathways, including the endoplasmic reticulum stress pathway, the JNK and NF $\kappa$ B signaling cascades, and apoptotic pathways (Hotamisligil and Erbay, 2008). As a result, metabolic pathways in hypertrophic adipocytes are repressed, mitochondrial functions decline, and insulin signaling is disrupted. Activation of stress pathways in adipocytes also attract macrophages that contribute to obesity-associated inflammation and insulin resistance (Guilherme et al., 2008; Lumeng and Saltiel, 2011).

Recently it was shown that the NLRP3 inflammasome is activated in white adipose tissue of obese mice and contributes to the progression of inflammation and insulin resistance (Vandanmagsar et al., 2011). NLRP3 inflammasome consists of the regulatory subunit NLRP3, the adaptor protein Asc, and the effector cysteine protease, caspase-1. Activation of the NLRP3 inflammasome leads to caspase-1-dependent cleavage of two members of the IL-1 family of cytokines, IL-1 $\beta$  and IL18 (Schroder and Tschopp, 2010). Importantly, mice lacking NLRP3 or caspase-1 are protected from high-fat diet-induced obesity, glucose intolerance, and adipose tissue inflammation (Stienstra et al., 2010; Vandanmagsar et al., 2011). However, how nutrient excess initiates and sustains inflammation still remains obscure. Understanding the molecular mechanisms that lead to repression of metabolic functions and activation of stress and inflammatory signals could be of value in fighting obesity and metabolic syndrome.

SIRT1 is a NAD<sup>+</sup>-dependent deacetylase that plays an important role in maintaining metabolic functions in many tissues counteracting obesity (Guarente, 2006). Transgenic mice that moderately overexpress SIRT1 in all tissues or mice treated with specific SIRT1 activators are protected from developing liver steatosis and insulin resistance after high-fat feeding (Banks et al., 2008; Bordone et al., 2007; Feige et al., 2008; Pfluger et al., 2008). The role of SIRT1 in adipocyte metabolism has been studied mostly with cell culture systems. In white adipocytes, SIRT1 inhibits differentiation by repressing the transcriptional activity of PPAR $\gamma$  (Picard et al., 2004) and improves insulin sensitivity by deacetylating NF $\kappa$ B (Yoshizaki et al., 2009). Whole-body deletion of SIRT1 impairs mobilization of free fatty acids from white adipose tissue in response to fasting (Picard et al., 2004). Also, a recent report showed an inverse relationship between SIRT1 levels in adipose tissue and inflammation in that tissue (Gillum et al., 2011).

In this report, using the Cre/loxP technology to specifically ablate *SIRT1* in differentiated adipocytes in vivo, we show that SIRT1 loss from adipose tissue results in a genetic reprogramming that largely overlaps with the reprogramming that occurs during high-fat diet feeding of wild-type mice. This finding prompted us to test the hypothesis that stress signals generated in obesity might inhibit SIRT1 activity in white adipose tissue. Indeed, we found that high-fat feeding or conditions of systemic inflammation induced the proteolytic cleavage of SIRT1. Importantly, our results show that NLRP3 inflammasome-activated caspase-1 is responsible for SIRT1 cleavage. This study establishes SIRT1 as an important link between stress signals

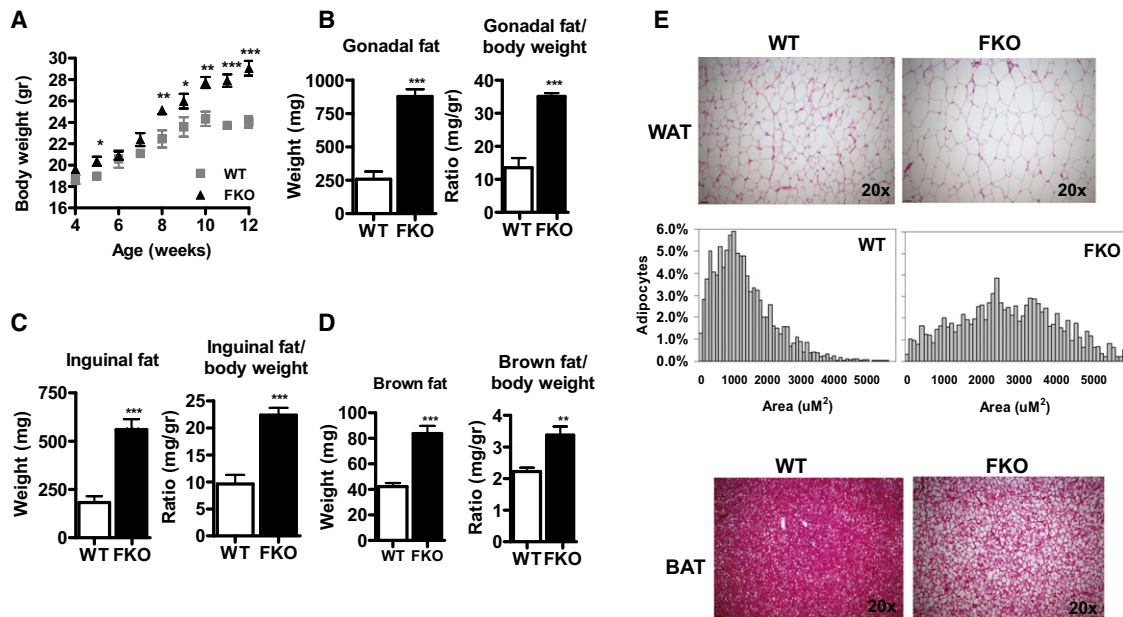


**Figure 1. SIRT1 Deletion from Adipose Tissue Leads to Obesity**

(A) Representative experiment of body weight gain of WT and FKO female mice on chow diet starting at 4 weeks of age ( $n = 5$ ).

(B–D) Gonadal, inguinal and brown fat mass of WT and FKO female mice at 2 months of age ( $n = 5$ ).

(E) Representative H&E staining of gonadal white adipose tissue and quantification of adipocyte size (500 cells/genotype,  $n = 3$ ).

All of the above experiments were repeated at least once, yielding the same conclusions. Data are expressed as mean  $\pm$  SEM. \* $p < 0.05$ , \*\* $p < 0.01$ , \*\*\* $p < 0.001$  by two-tailed unpaired Student's  $t$  test. See also Figure S1.

generated in adipose tissue during high-fat feeding and the metabolic dysfunction of the tissue.

## RESULTS

### Adipose Tissue-Specific SIRT1 Knockout Mice Have Increased Adiposity

To generate adipose tissue-specific *SIRT1* knockout (FKO) mice, we crossed mice carrying the conditional *SIRT1* allele (*SIRT1*<sup>fllox</sup>) to transgenic mice expressing the Cre recombinase under the control of fatty acid binding protein 4 promoter (*FABP4-cre*), which is strongly expressed in differentiated adipocytes (He et al., 2003). The *SIRT1*<sup>fllox</sup> mice contain loxP sites flanking exon 4 of the gene, which encodes part of the catalytic domain of the protein (Cheng et al., 2003). The excision resulted in the generation of a smaller, less stable and catalytically inactive SIRT1 protein, in both white and brown adipose tissue, as confirmed by western blot analysis (Figure S1A available online). We verified by genomic PCR and quantitative RT-PCR that the excision of exon 4 of *SIRT1* occurs strongly in mature adipocytes of *SIRT1* FKO mice and not in other nonadipocyte cells present in the adipose tissue, such as preadipocytes, fibroblasts, macrophages, and immune cells, collectively called stromal vascular fraction (SVF) cells (Figures S1B–S1D). Importantly, we verified that the excision did not occur in macrophages isolated from the bone marrow of *SIRT1* FKO mice (Figures S1A and S1C) or in the SVF fraction of adipose tissue of *SIRT1* FKO mice fed either chow diet or high-fat diet (Figures S1C and S1D). Moreover, we did not detect any significant expression of *Fabp4* in the SVF cells or macrophages by quantitative RT-PCR (Figures S1C and S1D).

*FABP4-cre; SIRT1*<sup>fllox/fllox</sup> (FKO) mice and *SIRT1*<sup>fllox/fllox</sup> wild-type (WT) littermate control mice were born at Mendelian ratios and appeared grossly normal. Interestingly, FKO mice fed chow diet gained significantly more weight compared to littermate WT controls over time (Figure 1A). The increased weight gain was manifested by increased accumulation of both visceral and subcutaneous fat. Gonadal and inguinal fat pads and brown adipose tissue from 2-month-old FKO mice fed chow diet weighed two to three times more compared to controls (Figures 1B, 1C, and 1D, respectively). Histological analysis of visceral adipose tissue from young adult mice showed that white adipocytes of FKO mice were enlarged and contained bigger lipid droplets compared to WT controls (Figure 1E). Similarly, brown adipose tissue appeared to contain more fat (Figure 1E). Consistent with the increased adiposity, plasma leptin levels (Figure S2A) were significantly higher in FKO compared to WT adult mice, while insulin (Figure S2B) and adiponectin (Figure S2C) levels were not significantly changed. The increased adiposity cannot be attributed to differences in free fatty acids or increased food intake, as we did not observe any significant difference between the two groups (Figures S2D and S2E, respectively). The increased body and adipose tissue weight, and the elevated plasma leptin levels were evident even in adolescent FKO mice (1 month old) (Figures S2F–S2H). In agreement with the normal levels of insulin and adiponectin in young adult FKO mice fed chow diet, glucose and insulin tolerance tests did not show any overt phenotype (Figure S2I). The increase in adiposity in FKO mice may be attributed to decreased metabolism in fat cells.

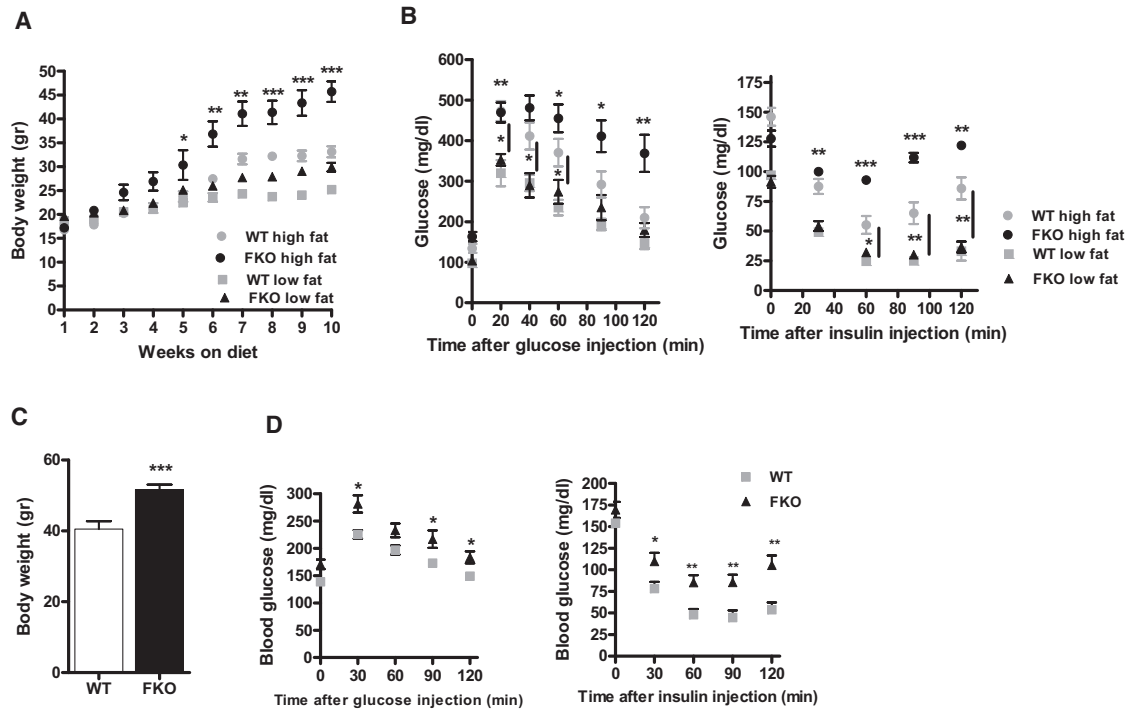


**Figure 2. SIRT1 Deletion from Adipose Tissue Results in Metabolic Deregulation**

(A) Weekly body weight of WT and FKO female mice on low-fat (LFD) and high-fat (HFD) diet.

(B) Glucose and insulin tolerance tests (GTT and ITT) of mice after 12 weeks on diet (n = 8).

(C and D) Body weight of aged WT and FKO female mice (~1 year old) (C) and glucose and insulin tolerance test (n = 10–12) (D).

The above experiments were repeated at least once, yielding the same conclusions. Data are expressed as mean ± SEM. \*p < 0.05, \*\*p < 0.01, \*\*\*p < 0.001 by two-tailed unpaired Student's t test. See also Figures S2 and S3.

### Adipose Tissue-Specific SIRT1 Knockout Mice Are Poised to Become Insulin Resistant

SIRT1 FKO mice have increased adiposity and leptin levels, which might indicate a predisposition to insulin resistance. To test this hypothesis, we challenged FKO and WT mice with a short-term high-fat diet (HFD) regimen, containing 60% calories from fat or control diet containing 10% calories from fat (low-fat diet [LFD]) for 12 weeks, starting after weaning. Interestingly, HFD caused a rapid increase of body weight (Figure 2A) and adipose tissue mass in FKO mice (Figures S3A–S3D), compared to the WT. This regimen elicited a mild metabolic dysfunction in WT mice (glucose and insulin tolerance tests, WT/LFD versus WT/HFD in Figure 2B), while this regimen caused severe glucose intolerance and insulin resistance in FKO (glucose and insulin tolerance tests, FKO/HFD versus WT/HFD in Figure 2B). The levels of leptin and insulin in FKO/HFD were significantly elevated compared to WT/HFD, in agreement with the overt metabolic phenotype (Figures S2A and S2B, respectively). Conversely, the adiponectin levels were significantly reduced in FKO/HFD correlating with its role as an insulin sensitizer (Figure S2C). FKO/HFD mice also had elevated circulating free fatty acids (Figure S2D), probably because of the increased adipose mass, and they consumed less food, probably as a response to the high levels of leptin (Figure S2E).

Next, we examined the effects of SIRT1 loss from adipose tissue in combination with aging. Interestingly, ~1-year-old FKO female mice fed chow diet presented a metabolic deregulation

similar to that of FKO/HFD mice. They weighed significantly more compared to WT littermates (Figure 2C) and were glucose and insulin intolerant, as shown by glucose (GTT) and insulin (ITT) tolerance tests (Figure 2D). They also had higher levels of plasma leptin (Figure S2A), insulin (Figure S2B), and free fatty acids (Figure S2D), and lower levels of adiponectin (Figure S2C). Thus, SIRT1 absence from adipose tissue leads to predisposition to diabetes, and when combined with a HFD or aging leads to a metabolic deregulation. These findings indicate that SIRT1 functions in adipose tissue to protect against metabolic deterioration upon dietary stress.

### Adipose SIRT1 Deletion and HFD Induce Very Similar Changes in Gene Expression

To examine the molecular mechanisms underlying the predisposition of FKO mice to obesity and high-fat diet-induced insulin resistance, we performed genome-wide expression profiling on RNA isolated from white adipose tissue (WAT) of four groups of mice: WT mice on low-fat diet (WT/LFD), WT mice on high-fat diet (WT/HFD), FKO mice on low-fat diet (FKO/LFD) and FKO on high-fat diet (FKO/HFD). As before, the mice were placed on this diet only for a short period of time (8 weeks).

We profiled 40,000 transcripts and performed hierarchical clustering of all transcripts assayed on the gene expression chip. A composite dendrogram showed that the four groups of mice formed three clusters, within which there was very little

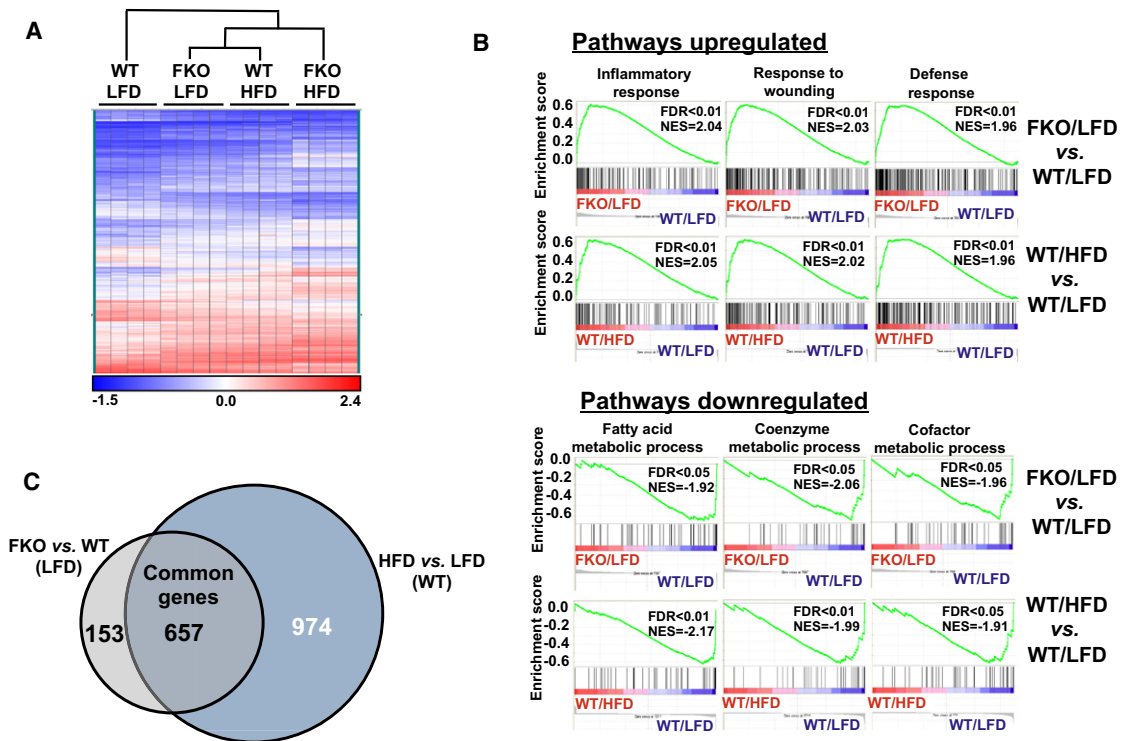


**Figure 3. Adipose SIRT1 Deletion and High-Fat Diet Induce Similar Changes in Gene Expression**

(A) Hierarchical clustering of samples based on changes in gene expression.

(B) Representative GSEA plots of gene pathways upregulated or downregulated in both the comparison FKO/LFD versus WT/LFD and WT/HFD versus WT/LFD are shown. Positive and negative enrichment scores indicate correlation and anticorrelation respectively. NES, normalized enrichment score; FDR, false discovery rate.

(C) Venn diagram of overlapping genes significantly changed ( $\pm 1.5$ -fold) in the comparisons FKO/LFD versus WT/LFD and WT/HFD versus WT/LFD.

See also Figure S4 and Table S1.

mouse to mouse variation: (1) WT/LFD, (2) FKO/HFD, and (3) WT/HFD and FKO/LFD (Figure S4A). A supervised hierarchical clustering using only the genes that changed at least 2-fold in any of the following comparisons, FKO/LFD versus WT/LFD, WT/HFD versus WT/LFD, and FKO/HFD versus WT/HFD, verified that FKO/LFD and WT/HFD shared a highly related gene signature (Figure 3A). We investigated further the association of FKO/LFD and WT/HFD by gene set enrichment analyses (GSEAs) of pathways most affected when comparing FKO/LFD versus WT/LFD and WT/HFD versus WT/LFD. The comparison of WT/HFD versus WT/LFD showed increases in gene categories related to inflammation (i.e., inflammatory response, response to wounding, and defense response) (Figure 3B and Table S1, part A) and decreases in categories related to metabolism (i.e., fatty acid metabolic process, coenzyme metabolic process and cofactor metabolic process) (Figure 3B and Table S1, part B). The comparison of FKO/LFD versus WT/LFD showed strikingly similar changes with the comparison WT/HFD versus WT/LFD, in most categories (Figure 3B and Table S1, parts A and B). The vast overlap between the genes changed in FKO/LFD versus WT/LFD and WT/HFD versus WT/LFD is shown in the Venn diagram (Figure 3C). These data indicate that deletion of SIRT1 in adipocytes elicits a set of transcriptional changes that is remarkably similar to the changes caused in adipocytes of WT mice fed a high-fat diet.

The fact that the FKO/HFD formed a cluster by itself (Figures 3A, S4A, and S4B) is consistent with the metabolic dysfunction unique to this group. Genes specifically induced in this group include those related to cell cycle and replication (Table S1, part D), which may arise from infiltrating macrophages and T cells (Nishimura et al., 2009; Yang et al., 2010). Indeed, RT-PCR analysis confirmed strong increases in messenger RNA (mRNA) levels of monocyte chemoattractant factor (*Mcp1*) and *Tnfa* that were unique to this group (Figure S4C). In conclusion, challenging FKO mice with HFD leads to whole body glucose intolerance that correlates with infiltration of replicating cells, possibly macrophages and T cells that respond to stress cues generated by the adipocytes.

Overall our gene expression analyses clearly show that genetic ablation of SIRT1 from adipose tissue causes changes in gene expression that largely overlap with the changes caused by HFD. We conclude that SIRT1 has important roles in maintaining metabolic functions of white adipose tissue, and protects against the deleterious effects of dietary stress.

#### High-Fat Diet Feeding Results in Reduced SIRT1 Levels, in White Adipose Tissue

Our gene expression analysis led us to hypothesize that HFD feeding might inhibit SIRT1 activity, mimicking the conditions of SIRT1 genetic ablation from adipose tissue. To test this

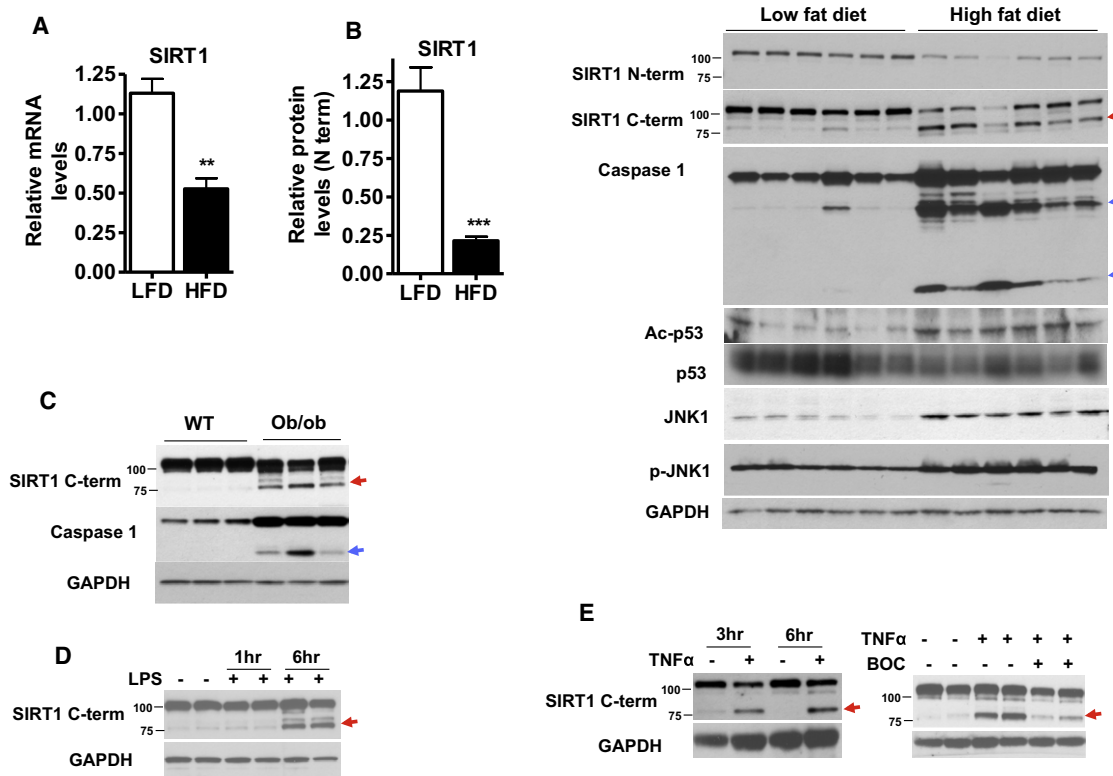


**Figure 4. Obesity and Inflammation Result in Reduced SIRT1 Activity in Adipose Tissue**

(A) Relative mRNA levels of *SIRT1* in adipose tissue of male mice fed low- or high-fat diet (males, n = 6). (B) Quantitative analysis of SIRT1 protein, using Image J software. Western blots of adipose tissue lysates from the same mice are shown. (C) Western blots in adipose tissue lysates prepared from WT and ob/ob male mice. (D) Western blot in adipose tissue lysates prepared from male mice treated with lipopolysaccharides for 1 hr and 6 hr. (E) Western blot in adipose tissue lysates prepared from male mice treated with TNF $\alpha$ , or combination of TNF $\alpha$  and the caspase inhibitor BOC-D-FMK (BOC). In all panels, red arrows indicate the cleaved form of SIRT1 and blue arrows indicate the active form of caspase-1. All of the above experiments were repeated at least once, yielding the same conclusions. Data are expressed as mean  $\pm$  SEM. \*\*p < 0.01, \*\*\*p < 0.001 by two-tailed unpaired Student's t test. See also Figure S5.

hypothesis, we examined whether HFD affects the levels of SIRT1. Quantitative RT-PCR analysis of RNA isolated from white adipose tissue showed that *SIRT1* mRNA levels were reduced by 2-fold in mice fed a HFD (Figure 4A). In addition, western blot analysis, using an antibody that recognizes the amino-terminal region of SIRT1 (1–131 aa) (Figure S6B), showed that protein levels were reduced almost 5-fold (Figure 4B). Western blotting of SIRT1 using a different antibody which recognizes the carboxy-terminal peptide of the protein (Figure S6B) revealed the presence of a faster migrating ~80 kD species in HFD lysates (Figure 4B, red arrow), which was undetectable by the amino-terminal antibody. Similarly, SIRT1 protein was reduced and the ~80 kD species was detected in WAT lysates from the genetically obese mice ob/ob (Figure 4C). These findings indicate that the full-length SIRT1 protein is proteolytically cleaved in adipose tissue of obese animals. In agreement with lower levels of active SIRT1, the acetylation levels of p53—a bona fide target of SIRT1—were elevated in adipose tissue from HFD mice (Figures 4B and S5B). The reduction of *SIRT1* mRNA levels is perhaps a result of feedback regulation of *SIRT1* on its own promoter (Nemoto et al., 2004; Xiong et al., 2011). Finally, the mRNA levels of *Nampt*, *Nmnat1*, and *Nmnat3*, key enzymes in the NAD

biosynthetic pathway, were downregulated in adipose tissue of HFD mice, a finding also consistent with lower SIRT1 activity (Figure S5A).

A mechanism that could explain the reduction of the full-length SIRT1 protein is its degradation by the proteasome machinery. In liver, dietary stress was shown to induce SIRT1 phosphorylation by activated phospho-JNK1 (Gao et al., 2011; Nasrin et al., 2009) and targeted for proteolysis (Gao et al., 2011). We tested whether JNK1 was activated in adipose tissue of mice fed HFD. Although we observed increased levels of both total JNK1 protein and the active, phosphorylated JNK1 in the HFD adipose tissue extracts (Figure 4B), we were unable to detect any phosphorylated SIRT1, using the phosphospecific antibody (Gao et al., 2011). While our data cannot exclude the possibility that SIRT1 protein is targeted by JNK1 for proteasomal degradation, the presence of the ~80 kD SIRT1 species, only detected by the carboxy-terminal antibody, points to a more specific proteolytic mechanism, that could be triggered by HFD.

To further explore this possibility, we queried which proteases might be responsible for SIRT1 cleavage. We used the ExPASy Proteomics Server (<http://ca.expasy.org/>) and the program PeptideCutter to search for consensus cleavage sites recognized by

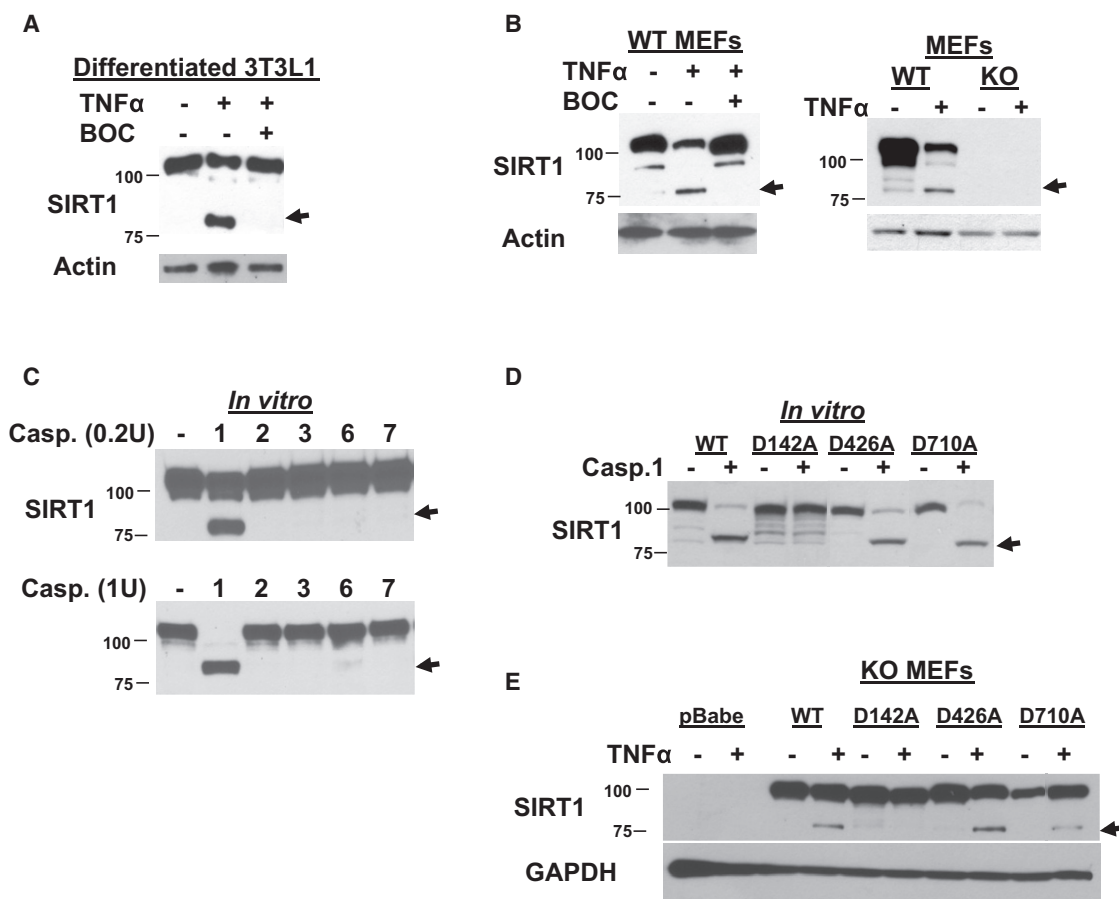


### Figure 5. Caspase-1 Cleaves SIRT1

(A) Western blot in whole cell extracts of differentiated 3T3L1 adipocytes treated with TNF $\alpha$  or combination of TNF $\alpha$  and the caspase inhibitor BOC-D-FMK (BOC). (B) Western blot in WT or *SIRT1* KO mouse embryonic fibroblasts lysates treated with TNF $\alpha$  or TNF $\alpha$  and BOC.

(C) Western blot in WT MEFs cell extracts treated *in vitro* with the indicated recombinant caspases.

(D) Western blot in extracts prepared from KO MEFs expressing WT or the indicated point mutant SIRT1 and treated *in vitro* with recombinant caspase-1.

(E) Western blot in extracts prepared from KO MEFs expressing WT or the indicated mutant SIRT1, treated with TNF $\alpha$ .

In all panels, arrows indicate the cleaved SIRT1 protein. All of the above experiments were repeated at least once, yielding the same conclusions. See also Figure S6.

known proteases. We identified three tetrapeptides in the mouse SIRT1 amino acid sequence predicted to be recognition sites for the cysteine proteases caspases, which cleave after an aspartic acid (Figure S6A). D142 and D710 were predicted as cleavage sites for caspase-1 and D426 for caspase-3/caspase-7. Interestingly, the NLRP3 inflammasome and the downstream effector protease caspase-1 were recently found to be activated in adipose tissue of WT mice fed a HFD and in ob/ob mice (Stienstra et al., 2010; Vandanmagsar et al., 2011), making caspase-1 an attractive candidate for SIRT1 cleavage. We confirmed that caspase-1 protein levels and activity are induced in WAT lysates of WT mice on HFD and of ob/ob mice, as indicated by the appearance of the cleaved, activated forms (Figures 4B and 4C, blue arrows).

Next, we tested whether SIRT1 cleavage is induced by pro-inflammatory signals that activate the NLRP3 inflammasome and caspase-1, irrespective of obesity (Tschopp and Schroder, 2010). Indeed, we observed cleavage of SIRT1 and production of the ~80 kD band in adipose tissue lysates of mice injected

with the proinflammatory compounds LPS (Figure 4D) or TNF $\alpha$  (Figure 4E). We verified that caspase-1 is activated under these conditions (Figures S5C and S5D). Importantly, this cleavage was prevented when the mice were pretreated with the general caspase inhibitor BOC-D-FMK, indicating that the proteolysis was caspase dependent (Figure 4E). In summary, these results suggest that the inflammatory signals associated with obesity promote a caspase-dependent cleavage of SIRT1 protein, resulting in whole-body metabolic dysfunction.

### Caspase-1 Is Responsible for SIRT1 Cleavage

We further investigated the molecular mechanism underlying the inflammation-induced SIRT1 cleavage, using cell culture systems. TNF $\alpha$  treatment of differentiated 3T3L1 adipocytes resulted in SIRT1 cleavage, generating a similar ~80 kD band as in adipose tissue (Figure 5A). This cleavage was prevented by pretreatment of the cells with the general caspase inhibitor BOC-D-FMK. We repeated this experiment using immortalized mouse embryonic fibroblasts (MEFs) from WT and *SIRT1*

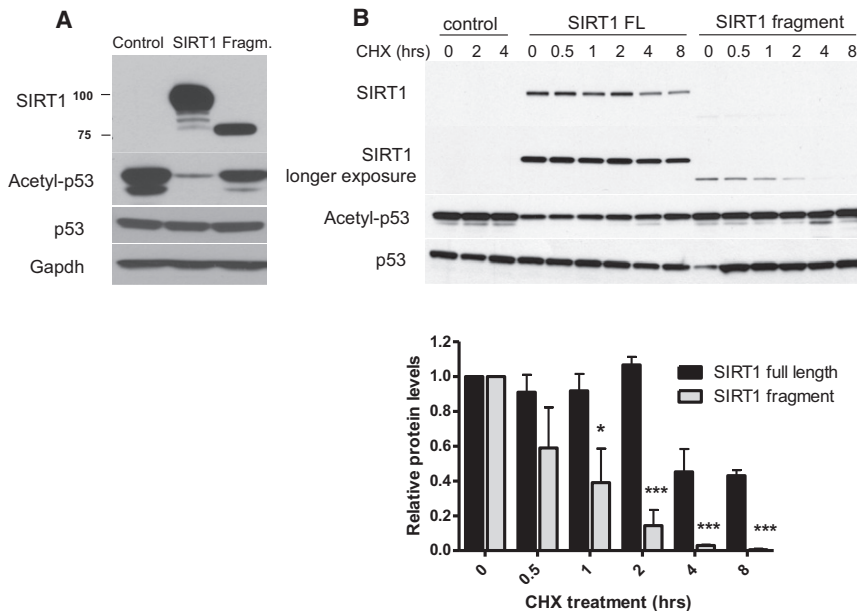


**Figure 6. Caspase-1 Cleaved SIRT1 Is Less Stable than Full-Length SIRT1**

(A) Western blot in whole-cell extracts of *SIRT1* KO MEFs transfected expressing the full-length SIRT1 or the truncated SIRT1 (fragment: D142-end) reveals a defect in p53 acetylation in cells transfected with truncated SIRT1.

(B) Western blot of cells treated with cyclohexamide (CHX) to inhibit protein synthesis for the indicated time. The graphs show the relative protein levels of full-length and truncated SIRT1 at time points after inhibition.

All of the above experiments were repeated at least once, yielding the same conclusions. Data are expressed as mean  $\pm$  SEM. \* $p < 0.05$ , \*\*\* $p < 0.001$  by two-tailed unpaired Student's *t* test.

## DISCUSSION

In this study we demonstrate that SIRT1 has an important role for the maintenance of metabolic functions in white adipose tissue and the prevention of the develop-

ment of obesity. Genetic ablation of *SIRT1* specifically from adipose tissue resulted in increased adiposity and predisposition to metabolic dysfunction. Gene expression studies and pathway analyses revealed that SIRT1 activity is necessary to protect adipose tissue from transcriptional changes that lead to obesity and a propensity to insulin resistance upon dietary stress. Strikingly, most of the transcriptional changes induced by a short-term HFD in WT mice were mimicked in the fat-specific *SIRT1* knockout mice fed a low fat diet. These findings suggest that HFD leads to SIRT1 inactivation in adipocytes, which is the cause of many of the resulting transcriptional changes.

Previous studies in liver indicate that stress signals trigger phosphorylation of SIRT1 by phosphorylated JNK1, leading to its destruction by the proteasome (Gao et al., 2011). In adipocytes, we observed that HFD leads to an increase in both total and active phosphorylated JNK1. This increase could explain part of the loss of SIRT1 activity, although we were unable to detect any phosphorylated SIRT1. However, our studies reveal a mechanism taking place in adipose tissue of HFD-fed mice: the proteolytic cleavage of SIRT1 by caspase-1, the effector protein of the NLRP3 inflammasome cascade. These findings are consistent with previous reports showing that the NLRP3 inflammasome is activated by HFD, and that knockout of caspase-1 protects against metabolic dysfunction on this diet (Stienstra et al., 2010; Vandanmagsar et al., 2011). Our findings suggest that the proinflammatory effect of the HFD is the triggering cue for SIRT1 cleavage. Indeed, other proinflammatory signals that activate caspase-1 via the NLRP3 inflammasome, such as TNF $\alpha$  also provoke the cleavage of SIRT1. Interestingly, PPAR $\gamma$ , a key metabolic regulator in adipose tissue, has been reported to be cleaved by caspases, under conditions of stress and inflammation (Guilherme et al., 2009; He et al., 2008). Therefore, the inflammasome-induced cleavage of key metabolic regulators, in the obese state might be the mechanism by which obesity-induced inflammation counteracts metabolic functions.

Next, we examined whether the cleavage of SIRT1 by caspase-1 in fact results in a reduction of SIRT1 function in cells. We overexpressed either the full-length or the truncated SIRT1 in *SIRT1* KO MEFs and determined the levels of acetylated p53. The deacetylase activity of the truncated SIRT1 on the acetylated p53 was reduced compared to the full-length SIRT1, but it was also expressed at lower steady state levels (Figure 6A). To determine whether truncated SIRT1 was degraded faster, we inhibited protein synthesis with cyclohexamide, and we measured the degradation rate of the full-length and the truncated SIRT1 proteins. The truncated SIRT1 was degraded much faster than the full-length protein (Figure 6B). From these data, we conclude that the caspase-1-mediated cleavage of SIRT1 reduces its activity, as the truncated protein is unstable and rapidly degraded.



In summary, our studies show that SIRT1 is necessary for the maintenance of metabolic health in adipose tissue under normal dietary conditions. Mice lacking SIRT1 are therefore predisposed to metabolic dysfunction upon dietary stress. Our findings lead to a two-stage model for the effects of HFD in WT mice. In the first stage, SIRT1 protein is at least partially inactivated in adipose tissue, causing a unique transcriptional profile and a predisposition to metabolic disease. Under prolonged metabolic stress, loss of SIRT1 function from adipose tissue leads to a diabetic phenotype, manifested by whole-body glucose intolerance and insulin resistance. Consistent with this model, FKO mice were predisposed to develop diabetes on a short-term HFD. However, the ability of SIRT1 to protect against dietary stress in WT animals is limited, because these animals lose SIRT1 and eventually become diabetic. It will be interesting to determine whether increasing SIRT1 activity in adipose tissue will confer metabolic protection against long-term high-fat feeding.

## EXPERIMENTAL PROCEDURES

### Animal Studies

All animal procedures were performed according to Massachusetts Institute of Technology Committee on Animal Care. All mice were in C57BL6/J genetic background. The analysis of FKO and WT littermates was performed in females, unless otherwise stated in the text. For diet studies, female mice were fed diets with 60% or 10% of calories from fat (high-fat diet and low-fat diet, respectively; Research Diets), starting at 4 weeks of age and for the 8–12 weeks as indicated in the text. For GTT and ITT, mice were fasted overnight prior to injection with either 1 g/kg glucose or 1 IU/kg insulin. Plasma insulin, leptin, and adiponectin levels were measured after overnight fasting, by ELISA kits (Millipore). Free fatty acids were measured after overnight fasting with a commercially available kit (WAKO). For the induction of acute inflammation, male or female mice were injected intraperitoneally with a combination of 5 mg/kg LPS (Sigma)/0.7 mg/kg GalN (Galactosamine-HCl, Sigma) or 0.1 mg/kg TNF $\alpha$  (Enzo life sciences)/ 0.7 mg/kg GalN. In some experiments 5 mg/kg BOC-D-FMK (Calbiochem) or vehicle was injected intraperitoneally 30 min prior to TNF $\alpha$ /GalN injection. LPS and TNF $\alpha$  treatments were done in both genders. Representative experiments performed in males are shown in the main text. Experiments in females are included in Figure S5.

### Histological Microscopy

Paraffin-embedded adipose tissue sections were stained with hematoxylin and eosin. The cross-sectional size (area,  $\mu\text{m}^2$ ) of adipocytes was determined in visceral adipose tissue with AxionVision software.

### Cell Culture

SIRT1 WT and KO mouse embryonic fibroblasts were previously described (Li et al., 2007). Mouse 3T3-L1 cells were cultured and differentiated toward adipocytes as described previously (Picard et al., 2004). For the TNF $\alpha$  treatment, cells were serum deprived overnight in Dulbecco's modified Eagle's medium (DMEM) containing fatty acid-free 0.3% bovine serum albumin. Next day they were treated with either 25  $\mu\text{g}/\text{ml}$  cycloheximide (CHX) alone (control), or followed by 50 ng/ml TNF $\alpha$  30 min later. In some experiments cells were pretreated for 1 hr with 50  $\mu\text{M}$  BOC-D-FMK followed by CHX and TNF $\alpha$ . Four hours after TNF $\alpha$  treatment, cells were washed and protein extracts were prepared. For retroviral infections, HEK293T cells were transfected with pBabe constructs. SIRT1 KO MEFs were infected with the viral particles produced, following standard procedures.

Macrophages were isolated from bone marrow from femurs and tibias and cultured in DMEM supplemented with 10% fetal calf serum and 20% L929 conditioned medium for 7 days. The medium was changed every 2 days.

### Stromal Vascular Cell Fraction and Macrophage Preparation

For the isolation of stromal vascular fraction (SVF) cells, adipose tissue was digested with collagenase (1 mg/ml) for 30 min at 37°C with shaking. The cell

suspensions were filtered through a 400  $\mu\text{m}$  nylon mesh and centrifuged at 500 g for 5 min. SVF pellets and infranatant adipocyte fraction were used for PCR analysis or RNA preparation.

### In Vitro Caspase Assays

WT MEFs or KO MEFs, expressing WT or mutant SIRT1 proteins, were lysed in 50 mM HEPES (pH 7.4), 50 mM NaCl, 0.1% Chaps, 1 mM EDTA, 5% glycerol, 10 mM DTT by sonication. Protein extracts (50  $\mu\text{g}$ ) were incubated with commercially obtained caspases (Calbiochem) at 37°C. The reaction was stopped with the addition of SDS buffer.

### Statistical Analysis

Data are expressed as mean  $\pm$  SEM. Statistical significance of the differences between groups was determined by two-tailed unpaired Student's t test with the GraphPad prism software (\*p < 0.05, \*\*p < 0.01, \*\*\*p < 0.001).

### ACCESSION NUMBERS

Gene expression data were deposited in Gene Expression Omnibus under accession number GSE30247.

### SUPPLEMENTAL INFORMATION

Supplemental Information includes Supplemental Experimental Procedures, six figures, and one table and can be found with this article online at <http://dx.doi.org/10.1016/j.cmet.2012.07.003>.

### ACKNOWLEDGMENTS

We thank C. Whittaker for the microarray data analysis, S. Nasamu for technical help, and K. Boulias, E. Bell, H.-C. Chang, and E. Williams for comments on the manuscript. A.C. was supported by a postdoctoral fellowship from American Heart Association. L.G. is supported by the NIH and the Glenn Foundation for Medical Research.

Received: July 7, 2011

Revised: March 4, 2012

Accepted: July 11, 2012

Published online: August 7, 2012

### REFERENCES

- Banks, A.S., Kon, N., Knight, C., Matsumoto, M., Gutiérrez-Juárez, R., Rossetti, L., Gu, W., and Accili, D. (2008). SirT1 gain of function increases energy efficiency and prevents diabetes in mice. *Cell Metab.* 8, 333–341.
- Bordone, L., Cohen, D., Robinson, A., Motta, M.C., van Veen, E., Czopik, A., Steele, A.D., Crowe, H., Marmor, S., Luo, J., et al. (2007). SIRT1 transgenic mice show phenotypes resembling calorie restriction. *Aging Cell* 6, 759–767.
- Cheng, H.L., Mostoslavsky, R., Saito, S., Manis, J.P., Gu, Y., Patel, P., Bronson, R., Appella, E., Alt, F.W., and Chua, K.F. (2003). Developmental defects and p53 hyperacetylation in Sir2 homolog (SIRT1)-deficient mice. *Proc. Natl. Acad. Sci. USA* 100, 10794–10799.
- Feige, J.N., Lagouge, M., Cantot, C., Strehle, A., Houten, S.M., Milne, J.C., Lambert, P.D., Matak, C., Elliott, P.J., and Auwerx, J. (2008). Specific SIRT1 activation mimics low energy levels and protects against diet-induced metabolic disorders by enhancing fat oxidation. *Cell Metab.* 8, 347–358.
- Gao, Z., Zhang, J., Kheterpal, I., Kennedy, N., Davis, R.J., and Ye, J. (2011). Sirtuin 1 (SIRT1) protein degradation in response to persistent c-Jun N-terminal kinase 1 (JNK1) activation contributes to hepatic steatosis in obesity. *J. Biol. Chem.* 286, 22227–22234.
- Gillum, M.P., Kotas, M.E., Erion, D.M., Kursawe, R., Chatterjee, P., Nead, K.T., Muise, E.S., Hsiao, J.J., Frederick, D.W., Yonemitsu, S., et al. (2011). SirT1 regulates adipose tissue inflammation. *Diabetes* 60, 3235–3245.
- Guarente, L. (2006). Sirtuins as potential targets for metabolic syndrome. *Nature* 444, 868–874.

- Guilherme, A., Virbasius, J.V., Puri, V., and Czech, M.P. (2008). Adipocyte dysfunctions linking obesity to insulin resistance and type 2 diabetes. *Nat. Rev. Mol. Cell Biol.* **9**, 367–377.
- Guilherme, A., Tesz, G.J., Guntur, K.V., and Czech, M.P. (2009). Tumor necrosis factor- $\alpha$  induces caspase-mediated cleavage of peroxisome proliferator-activated receptor gamma in adipocytes. *J. Biol. Chem.* **284**, 17082–17091.
- He, W., Barak, Y., Hevener, A., Olson, P., Liao, D., Le, J., Nelson, M., Ong, E., Olefsky, J.M., and Evans, R.M. (2003). Adipose-specific peroxisome proliferator-activated receptor gamma knockout causes insulin resistance in fat and liver but not in muscle. *Proc. Natl. Acad. Sci. USA* **100**, 15712–15717.
- He, F., Doucet, J.A., and Stephens, J.M. (2008). Caspase-mediated degradation of PPARgamma proteins in adipocytes. *Obesity (Silver Spring)* **16**, 1735–1741.
- Hotamisligil, G.S., and Erbay, E. (2008). Nutrient sensing and inflammation in metabolic diseases. *Nat. Rev. Immunol.* **8**, 923–934.
- Li, X., Zhang, S., Blander, G., Tse, J.G., Krieger, M., and Guarente, L. (2007). SIRT1 deacetylates and positively regulates the nuclear receptor LXR. *Cell* **28**, 91–106.
- Lumeng, C.N., and Saltiel, A.R. (2011). Inflammatory links between obesity and metabolic disease. *J. Clin. Invest.* **121**, 2111–2117.
- Nasrin, N., Kaushik, V.K., Fortier, E., Wall, D., Pearson, K.J., de Cabo, R., and Bordone, L. (2009). JNK1 phosphorylates SIRT1 and promotes its enzymatic activity. *PLoS ONE* **4**, e8414.
- Nemoto, S., Fergusson, M.M., and Finkel, T. (2004). Nutrient availability regulates SIRT1 through a forkhead-dependent pathway. *Science* **306**, 2105–2108.
- Nishimura, S., Manabe, I., Nagasaki, M., Eto, K., Yamashita, H., Ohsugi, M., Otsu, M., Hara, K., Ueki, K., Sugiura, S., et al. (2009). CD8+ effector T cells contribute to macrophage recruitment and adipose tissue inflammation in obesity. *Nat. Med.* **15**, 914–920.
- Pfluger, P.T., Herranz, D., Velasco-Miguel, S., Serrano, M., and Tschöp, M.H. (2008). Sirt1 protects against high-fat diet-induced metabolic damage. *Proc. Natl. Acad. Sci. USA* **105**, 9793–9798.
- Picard, F., Kurtev, M., Chung, N., Topark-Ngarm, A., Senawong, T., Machado De Oliveira, R., Leid, M., McBurney, M.W., and Guarente, L. (2004). Sirt1 promotes fat mobilization in white adipocytes by repressing PPAR-gamma. *Nature* **429**, 771–776.
- Qatanani, M., and Lazar, M.A. (2007). Mechanisms of obesity-associated insulin resistance: many choices on the menu. *Genes Dev.* **21**, 1443–1455.
- Rosen, E.D., and Spiegelman, B.M. (2006). Adipocytes as regulators of energy balance and glucose homeostasis. *Nature* **444**, 847–853.
- Schroder, K., and Tschopp, J. (2010). The inflammasomes. *Cell* **140**, 821–832.
- Stienstra, R., Joosten, L.A., Koenen, T., van Tits, B., van Diepen, J.A., van den Berg, S.A., Rensen, P.C., Voshol, P.J., Fantuzzi, G., Hijmans, A., et al. (2010). The inflammasome-mediated caspase-1 activation controls adipocyte differentiation and insulin sensitivity. *Cell Metab.* **12**, 593–605.
- Tschopp, J., and Schroder, K. (2010). NLRP3 inflammasome activation: The convergence of multiple signalling pathways on ROS production? *Nat. Rev. Immunol.* **10**, 210–215.
- Vandanmagsar, B., Youm, Y.H., Ravussin, A., Galgani, J.E., Stadler, K., Mynatt, R.L., Ravussin, E., Stephens, J.M., and Dixit, V.D. (2011). The NLRP3 inflammasome instigates obesity-induced inflammation and insulin resistance. *Nat. Med.* **17**, 179–188.
- Xiong, S., Salazar, G., Patrushev, N., and Alexander, R.W. (2011). FoxO1 mediates an autocrine feedback loop regulating SIRT1 expression. *J. Biol. Chem.* **286**, 5289–5299.
- Yang, H., Youm, Y.H., Vandanmagsar, B., Ravussin, A., Gimble, J.M., Greenway, F., Stephens, J.M., Mynatt, R.L., and Dixit, V.D. (2010). Obesity increases the production of proinflammatory mediators from adipose tissue T cells and compromises TCR repertoire diversity: implications for systemic inflammation and insulin resistance. *J. Immunol.* **185**, 1836–1845.
- Yoshizaki, T., Milne, J.C., Imamura, T., Schenk, S., Sonoda, N., Babendure, J.L., Lu, J.C., Smith, J.J., Jirousek, M.R., and Olefsky, J.M. (2009). SIRT1 exerts anti-inflammatory effects and improves insulin sensitivity in adipocytes. *Mol. Cell. Biol.* **29**, 1363–1374.